

Ruby Analysis via Spectroscopy Systems

Atman Atman, Brianna Hurrell, Brandon Lopez,
Isabelle Lebron^[God]

Dept. of Electrical Engineering and Computer
Science and CREOL, The College of Optics and
Photonics, University of Central Florida,
Orlando, Florida, 32816-2450

Abstract — This paper presents the design process utilized to develop a proof of concept system that determines whether a ruby is real, whether that be synthetic or natural, or an imitation, such as garnet or dyed quartz, through spectroscopy methods. The project utilizes two separate tests with both spectrums analyzed to determine the validity of the ruby. These tests analyze the dichroic properties of the ruby, a property determined by the output spectrum of the crystal structure, and the fluorescence, a material property of corundum with a dopant. This was done with the implementation of electrical, optical, and software components that will be detailed within this paper. The ruby is placed into a holder and light is shone onto it in two separate tests.

Index Terms — Dichroism, Spectrometer, Spectroscopy, Ruby, Fluorescent

I. INTRODUCTION

The idea behind this device was conceived to assist layman gem consumers in purchasing gems of unknown origin. The field of crystallography, which is essential to confirming the genuineness of gemstones, has made significant strides recently. But the abundance of lab-created gems has increased demand for more accurate and reliable distinguishing techniques. There is a growing consensus in response to this critical problem that a flexible system is needed in order to combine different approaches into a single platform and minimize human errors and personal biases in gemstone authentication procedures. The main goal of this kind of system is to create a prototype that can reliably differentiate between real and fake rubies. Using spectroscopy techniques, this integrated system carefully analyzes the distinct aspects of rubies.

The system Ruby Analysis via Spectroscopy Systems, known as RASS, is a device designed in order to utilize both fluorescence spectroscopy and the dichroic properties of gemstones in order to determine if a ruby is real, whether that be synthetic or natural, or an imitation. This is a proof of concept design that can later be tailored to

other gems such as diamond or sapphire. The design of the RASS involves a bridge rectifier PSU board, a regulator PSU board, a ruby mounting system with a laser and LED input that leads into a lens system output that is read by the spectrometer that operates on a Raspberry Pi module and HQ camera.

Rubies have very specific properties that can be tested for. They have trigonal crystal structures that exhibit dichroism, the splitting of reflected or transmitted light into two distinct visible wavelengths, due to the crystal lattice's structure and orientation. These wavelengths should appear red and pink to the human eye, and thus a spectrometer can test for them. In addition, rubies exhibit fluorescence at a specific wavelength of 550 nm due to the chromium dopant that gives rubies their distinct red color. Rubies that don't fluoresce or do so at the wrong wavelength can be determined to be fake.

RASS aims to harness these properties by employing distinct light sources in two separate tests. This will enable precise observation and recordings of the color changes that happen within each test that can be used to determine whether the presented ruby is genuine.

II. SYSTEM COMPONENTS

First the electrical then optical components of the system will be explored. How they coincide with each other will be examined in future parts.

A. Step Down Transformer

A total of 120 VAC is supplied to the transformer which is then stepped down to around ~13 VAC RMS. This voltage is then supplied to a bridge rectifier which in turn produces approximately ~17 VDC.

B. Bridge Rectifier PSU Board

This board supplies energy to both LEDs and the Raspberry Pi 3. The Raspberry Pi 3 requires 5 volts of energy. Both the white LED and the green LED require approximately 2 to 3 volts. This rectifier supplies ~17 VDC to an LM2576 voltage regulator. This regulator then supplies 5V to both the Raspberry Pi subsystem and the LED subsystem.

We have designed the LED branches to accommodate distance away from the board. This allows for better handling and maneuverability of the LEDs. This type of configuration also made using the LEDs with this PCB more efficient. This configuration also excludes the transformer from this board for increased maneuverability.



Fig. 1. Power supply unit for micro-USB and LEDs

The bridge rectifier sends 4A current or energy to a LM2576 voltage regulator. The LM2576 then supplies energy (3A) to both the Raspberry Pi subsystem and the LED subsystem. It was noted that there was approximately 0.02 V lost across the wire that connects the micro USB connector to the Raspberry Pi. This caused the signal from the Raspberry Pi to the monitor to be dropped after approximately 45 seconds. This was solved by designing a wire of a lower gauge (AWG 14) and accounting for the type of power loss. It was noted that the voltage loss was reduced dramatically using this method.

C. Regulator PSU Board

This board supplies energy to both the microcontroller unit (MCU) board and the servo motor, 3.3V and 5V respectively. Here, a different LM2576 voltage regulator is used to supply 5 volts. This 5V is supplied to a low dropout (LDO) voltage regulator which is used to lower the 5 volts to 3.3 volts. This 3.3V is then used to supply energy to the MCU board.



Fig. 2. Power supply unit for MCU and servo motor

D. Microcontroller (MCU) Board

The MCU board's main functions are to govern the signals that are used to make both the motor and potentiometer function, to supply energy to the potentiometer, and to connect both the motor and potentiometer to common. It is designed without any emulation capabilities as we are only interested in controlling the signals and power of a servo motor with a potentiometer. The input voltage to the MCU is 3.3 volts. The governing IC that is programmed on this board is the MSP-EXP430G2553. Note that this board supplies voltage to the potentiometer which uses 1 volt to 3.3 volts. It also supplies voltage to the IC (3.3V).

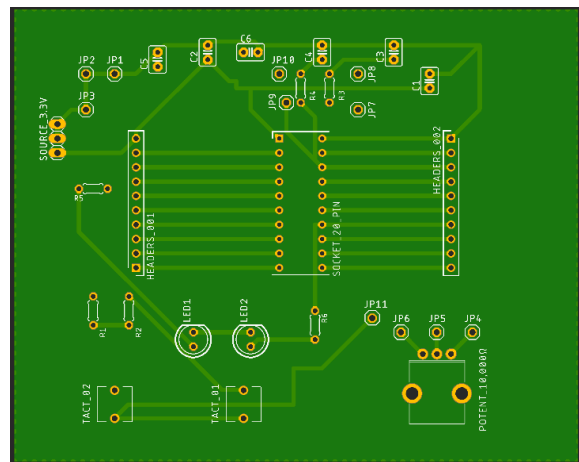


Fig. 3. Microcontroller unit (MSP-EXP430G2553)

E. Servo Motor and Potentiometer

The use of these two devices requires that the MCU be programmed to send signals to the specific signal pins or bits where these devices are connected, namely BIT3 and BIT6. The voltage requirements are listed in the preceding paragraphs.

F. Raspberry Pi 3

One of the key advantages of Raspberry Pi is its ability to run a full-fledged operating system (OS) like Raspberry Pi OS, based on Linux. This enables it to perform a wide range of tasks, from serving as a basic desktop computer to running web servers and media centers. Raspberry Pi also features built-in support for wireless connectivity via Wi-Fi and Bluetooth.

The Raspberry Pi 3 is used for the project and stands out as the optimal choice due to its image processing capabilities. Leveraging its versatile hardware and software ecosystem, the Raspberry Pi enables efficient image capture and processing. This is crucial when it

comes to analyzing diffraction gratings. Its computational power, coupled with libraries like OpenCV, allows for pattern recognition and spectral analysis directly on the device.

Raspberry Pi runs a full-fledged operating system, typically a variant of the Linux kernel. This allows it to support a wide range of programming languages and software development tools. Python, in particular, is the de facto programming language for Raspberry Pi, making it an excellent choice for both beginners and experienced developers. It can run web servers, databases, and other software applications. The ability to run a full operating system also enables multitasking and the use of graphical user interfaces, making Raspberry Pi suitable for projects that require user interaction. Additionally, you can install various Linux-based software packages, which opens up opportunities for diverse applications[1].

G. HQ Camera

The Raspberry Pi HQ Camera, paired with the Arducam lens, provides an optimal solution for capturing diffraction grating images. The HQ Camera's high resolution and compatibility with the Raspberry Pi ecosystem ensure detailed image capture, while the wide-angle lens and manual focus allow for precise adjustment and comprehensive coverage of diffraction patterns. Together, these components enhance translational accuracy and facilitate reliable spectral analysis, making them an ideal choice for spectroscopic applications.

H. Ruby Samples

To properly test the RASS, both a synthetic (real) ruby and fake (imitation, dyed quartz) ruby were used. These samples were sourced from reputable sellers, and their properties are tested using the methods employed by RASS as proof of the device working.

I. Light Sources

After much testing and deliberation, it was decided that a green laser that emits at the needed fluorescing wavelength of 550 nm would be used for the fluorescent testing in addition to a bright enough white LED for the dichroism measurements. While going through the testing of the RASS it was determined that green LEDs on the market did not have adequate light output to fluoresce the ruby enough to get readings from the spectrometer.

J. Lens System

The focusing system is composed of multiple parts. Arguably the most important of these parts is the concave mirror, that captures the light that transmits through the ruby and reflects it back into the lens system. Without this crucial component, most light projected onto the ruby would be absorbed into the housing and would not

contribute to the readings, risking too low intensities for effective spectrometer measurements.

Each lens within the system was chosen carefully to maximize light input into the spectrometer. The first lens is purposefully large with as short of a focal length as could be managed on a limited budget in order to take the strongly diverging light and collimate it as much as possible. It was necessary that this be large due to the reflections of light from the back facets of the gem, which are typically cut anywhere from 30 to 65 degrees depending on the type of cut. More intense angles will cause the reflected light to diverge more rapidly, making it harder to collect for smaller lenses. The second lens was also chosen to be larger, as the light from the first lens is focused more but not perfectly, so this lens was placed to make up for it. Post this second lens the spot size was below that of an inch and a half, so standard sized lenses could be used. Many of these lenses were chosen in accordance with both our budget and our spot size needs. There used to be more components in the system to reduce the spot size further, but those were removed due to the losses due to Fresnel reflections at each surface and the increased size it would add to the system.

K. Spectrometer

In designing the Ruby Analysis via Spectroscopy System (RASS), a crucial part is how to quantitatively measure the fluorescent light emitting from the ruby we chose to make a spectrometer. The RASS has a Czerny-Turner spectrometer.

Known for its measurement of intensity at various wavelengths the Czerny Turner spectrometer is a versatile and widely utilized tool in spectroscopy. It typically comprises three elements; an entrance slit, a diffraction grating and a detector. Light enters from a source through the entrance slit. Gets collimated by a mirror or lens. This collimated light then hits the diffraction grating, where it separates into wavelengths. Subsequently the dispersed light is directed onto a detector using another mirror or lens. By adjusting either the detector's position or the diffraction gratings angle this spectrometer can analyze intensity across a wavelength range proving beneficial in fields like chemical analysis, material characterization and astronomy.

The Czerny Turner spectrometer boasts advantages such as spectral resolution, flexibility in selecting wavelengths and capability to measure both emission and absorption spectra. Its modular structure allows for customization and optimization tailored to needs. Furthermore the progress in technology has resulted in the creation of sturdy spectrometers that're suitable for use in portable and field settings. However certain obstacles like light, optical alignment and calibration need to be addressed when setting up and operating these devices. Despite these

challenges, the Czerny-Turner spectrometer remains a cornerstone tool in both research and industrial settings, facilitating precise and accurate measurements of light spectra across diverse fields of study. Its versatility and reliability make it indispensable for scientists and engineers seeking to analyze and understand the intricate properties of light-emitting substances like rubies

III. SYSTEM CONCEPT

To understand the system as a whole, a flow chart has been added in Fig. *INSERT NUMBER HERE*

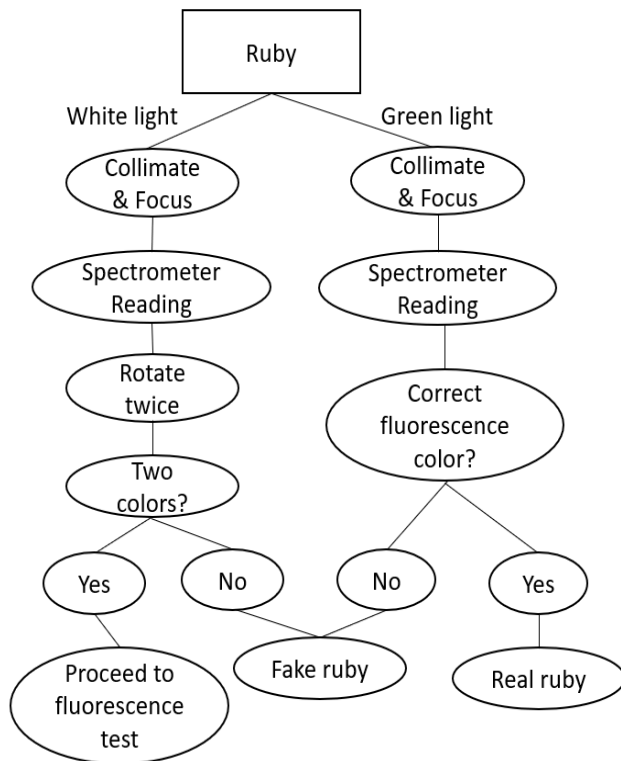


Fig. 4. A flow chart of RASS overall goal to enhance user understanding.

As can be garnered from the above diagram, the RASS will feature two tests. The first one will be the dichroism test, where white light will be shone onto the ruby and anything transmitted and reflected will be fed back through the focusing system, where the spot size of the system will be reduced down to allow for maximum light into the spectrometer. The spectrometer will then spread the light into its constituent wavelengths that will shine onto a screen and be read by the Pi camera. The second test will have a green laser fluorescing a ruby looking for a specific wavelength of 694 nm. If the ruby fails either of

these tests, it is deemed a fake ruby and the results will be reported to the user.

A. Image Capturing

The application of OpenCV's feature detection and image processing capabilities facilitates the extraction of the diffraction pattern with remarkable fidelity. Notably, the clarity and contrast of the diffraction pattern are significantly improved in the processed image compared to the raw capture.

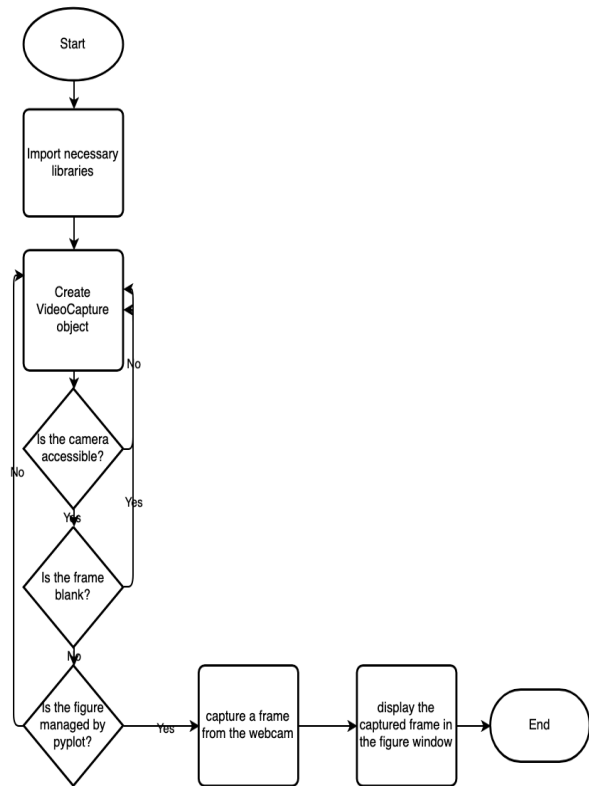


Fig. 5. Flowchart for capturing the spectra

The utilization of OpenCV enables efficient removal of noise and artifacts from the captured image, thereby enhancing the accuracy of subsequent spectral analysis. By leveraging OpenCV's functionalities, researchers can effectively extract valuable spectral information from the diffraction grating images, paving the way for precise and reliable analysis. The processed image demonstrates the efficacy of OpenCV in capturing and enhancing diffraction grating images for spectral analysis applications.

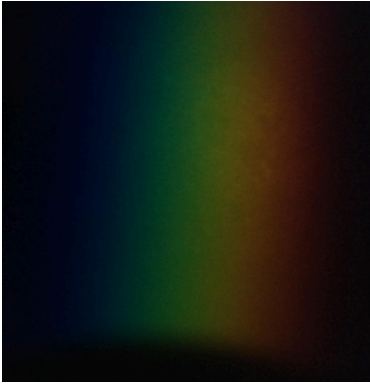


Fig. 6. The figure shows an example of spectra captured by the Pi Camera of white light with the System.

B. Graph Conversion

In the project, the HQ camera is utilized to capture a frame and then plots the value of the pixels that has been read along a chosen row of the image. Utilizing an empty NumPy array, the values at the specified row are saved for later use. A loop iterates over the x range, capturing RGB values at the position. The goal plottable value is calculated by averaging the read RGB values, then added to the array. Normalization is performed by subtracting the minimum value from the spectrum. Finally, the spectrum is plotted, and script execution is halted until the figure window is closed.

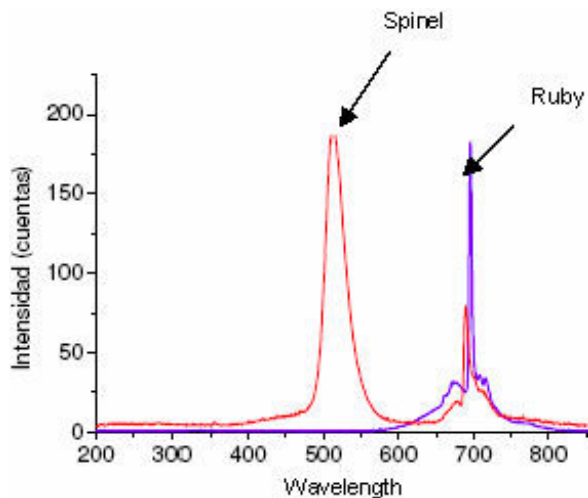


Fig. 7. A graph comparing the spectra of Ruby and Spinel.

C. Peak Detection

The objective of the algorithm is to detect peaks within designated data ranges. From this it can be ascertained whether the material being analyzed is a Ruby based on the presence of the characteristic peaks.

A set of ranges is defined at the start of the algorithm which are readily available for subsequent use, although for the purpose that we are searching for a singular range spanning from 690 to 700 is utilized.

Within the algorithm, a function call is made, accepting three arguments: 'x_vals' (representing x-axis data), 'y_vals' (denoting y-axis data), and 'ranges' (indicating the ranges to search within) for the 'find_peaks_in_ranges' function. It iterates through each specified range.

Utilizing the 'find_peaks' function from SciPy, peaks within each range are identified. The x and y values of the identified peaks are retrieved using their respective peak indices.

As can be seen from Figure 1, the expected characteristic peaks are within the range that is being tested for. When compared to a similar material, such as spinel, the ruby is differentiated by these characteristics.

The condition evaluates whether any peaks are detected within the specified ranges for the provided x and y data. If peaks are detected, it returns True, indicating the presence of a "Ruby"; conversely, it returns False, suggesting that it is not a "Ruby."

SciPy is utilized for the scientific and technical computing tasks, serving as a valuable extension to NumPy. Within its submodules there are tools for interpolation, solving differential equations, Fourier transforms, and specialized mathematical functions important in scientific research, engineering simulations, and data analysis. The ease of integration with other scientific libraries made it the preferred choice for the mathematical operations. This library was the primary resource utilized when analyzing the peaks of the data.

IV. HARDWARE DETAIL

The components explained above will now be illustrated within their intended system. In addition, the diode and regulator correspondence will be explored in further detail.

A. Hardware Concept

The overall system diagram gives an overview of how every component in the system works together. The individual light sources shine upon the ruby housed on a rotating stage. The stage is rotated through an MCU and the different light outputs are passed through a focusing system that maximizes output into the spectrometer. The quantitative results of the spectrometer are read by the HQ camera that's programmed by the Pi module then displayed externally. The overall hardware concept as well can be seen in Figure 8.

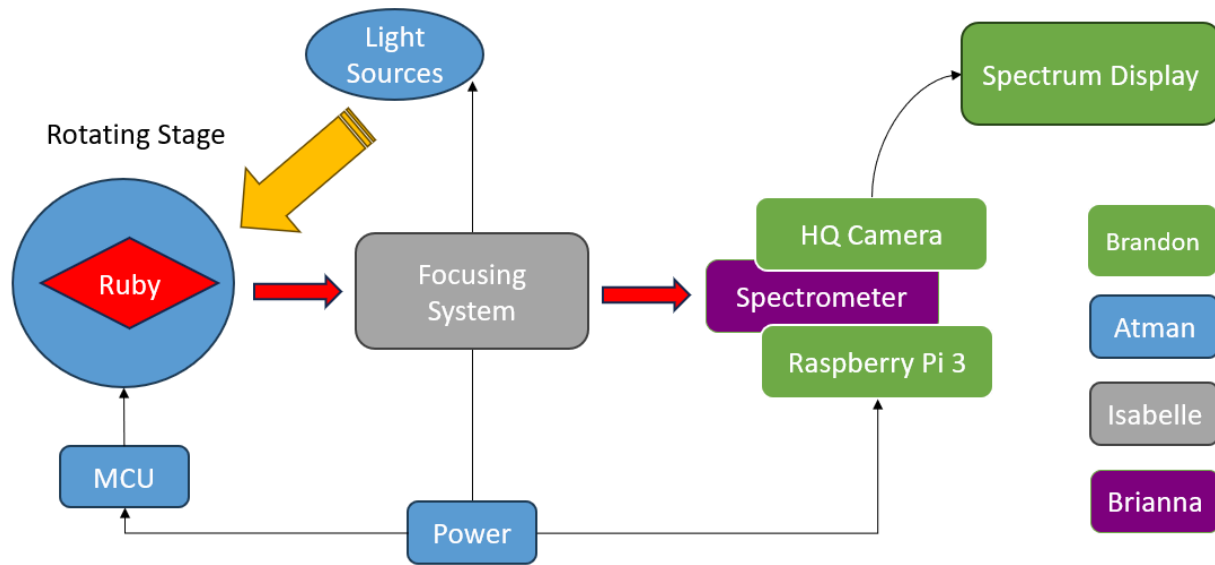


Fig. 8. Overall hardware schematic with color coded team member assignments.

B. Lens System

The first component of the lens system is the concave mirror behind the ruby. This was selected to have a focal length of 50 mm due to availability of parts. Ideally a shorter focal length would've been chosen to enable less divergence of rays as they enter the system. Due to this being unavailable, it was compensated by allowing room for the LED and picking a larger initial lens with a diameter of 5 inches and a focal length of 100 mm. It was placed 25 mm away from the ruby to allow for room for the input light while still allowing maximum light output. The next lens had a diameter of three inches and a focal length of 50 mm and was placed 80 mm away from the first lens. A mirror was placed where the spot size was near its smallest, at around 25 mm, and angled so that the beam path would enter the next pair of 20 mm FL lenses.

It is worth noting that the initial design utilized the versatility of conventional 4f systems when guiding light along a desired path. However, after extensive testing of this design and removing or switching out components, it was found that rather than adhering to the very specific focal lengths given in specifications, better results could be achieved when adjusting each individual lens within the system and studying their interactions with each other. Taking it systematically rather than placing them at predetermined distances yielded the best results. Distances were then recorded after measuring and implemented into Figure 9.

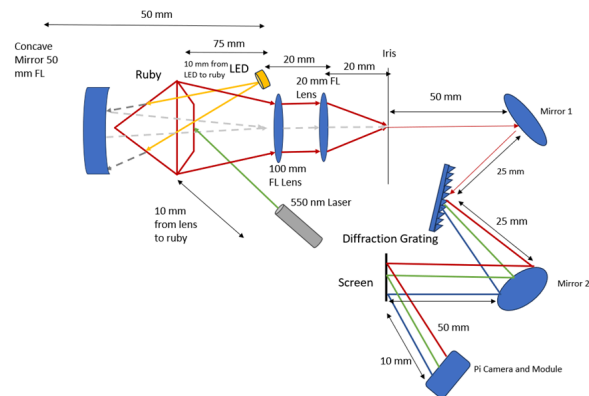


Fig. 9. The diagram that outlines the overall lens system that RASS utilizes.

C. Spectrometer

Key considerations revolve around the width of the slit and the type of dispersion element used. The slit, which allows fluorescence excited light to exit, plays a role in determining resolution. A wider slit provides power potentially reducing the time needed for accurate readings. [2] On the other hand a narrower slit expands the bandwidth of the absorption spectrum. For instance a 250 μm slit width was chosen for RASS based on equation 1 calculations involving factors like the distance between the slit and image as the maximum transmittance wavelength at 694 nm.

$$t = 1.9\sqrt{d} \times \lambda \quad (1)$$

When it comes to dispersion optics selection there is usually a choice between using a diffraction grating or a prism. While prisms offer benefits such as customization options they can be challenging to obtain for smaller scale projects. Therefore RASS opts for a diffraction grating due to its availability and effectiveness.

Diffraction gratings play a role in sorting and examining light by breaking it down into wavelengths allowing for the analysis of spectral patterns. These tools are components of spectrometers aiding in the measurement and assessment of intensity across varying wavelengths. [2]

The functioning of diffraction gratings is based on wave interference principles, where positioned grooves interact with light to scatter it into distinct wavelengths. This interaction leads to the creation of patterns through the destructive interference between primary light waves and secondary waves. Different diffraction orders represent diffracted light from perspectives corresponding to wavelengths. Ruled and holographic gratings are both vital in spectrometers, each offering benefits regarding durability, optical precision and wavelength coverage.

Factors like groove spacing, diffraction angle and blazed angle are crucial for designing and utilizing spectrometers. Groove spacing dictates dispersion and the spectrum of wavelengths while diffraction and blazed angles enhance grating efficiency, for desired wavelength ranges. The RASS will be utilizing a 300 grooves/mm ruled reflective diffraction grating. With that in mind in order to design the spectrometer the equation:

$$\sin(\theta_m) = \frac{m\lambda}{a} + \sin(\theta_i) \quad (2)$$

In order to calculate the diffraction angle with various angles of incidence, shown in Table 1.

TABLE I
INCIDENT ANGLE VS. DIFFRACTION ANGLE

θ_m when $\theta_i =$	300 grooves/mm
$\theta_i = 15^\circ$	27.85°
$\theta_i = 30^\circ$	45.11°
$\theta_i = 45^\circ$	66.28°

The final design of the RASS spectrometer is shown in Figure 10. As shown the angle of incidence is 15° and the diffraction angle is 27.85°.

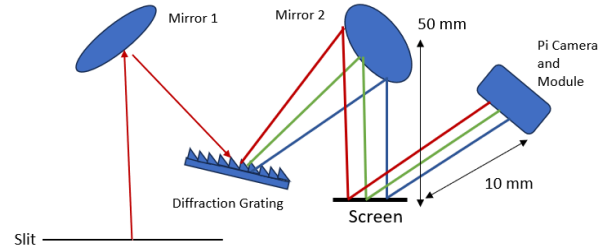


Fig. 10. The diagram that outlines the RASS spectrometer in a Czerny Turner style

D. Diode & Regulator Correspondence

One of the critical configurations of our PSU is how the LM2576 voltage regulator is engaged with and through the PE-92105 power inductor. The significance of this is that the power inductor stores energy in the form of a magnetic field when current flows through it. This stored energy is then released when the current through the inductor decreases. This inductor helps smooth out the output voltage by filtering out ripples and noise. As the inductor stores and releases energy, it tends to smooth out variations in the output voltage caused by changes in load or input voltage.

Inductors resist changes in current flow. This characteristic helps to limit the rate of change of current flowing through the circuit, which is particularly important in switching regulators like the LM2576. It prevents sudden spikes in current, thereby reducing stress on other components and ensuring stable operation. With the LM2576 voltage regulator, the power inductor is typically part of the switching circuit. It works in conjunction with the Schottky diode to regulate the output voltage efficiently[3].

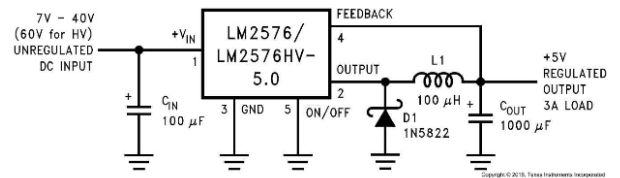


Fig. 11. Configuration of power inductor, Schottky diode, & regulator [3]

This power inductor is rated at 145 µH. Higher inductance values usually result in lower switching frequencies, while lower inductance values lead to higher switching frequencies. The choice of switching frequency impacts factors such as component size, efficiency, and electromagnetic interference (EMI).

The input voltage across the inductor depends on the duty cycle of the switching regulator and the input voltage

of the circuit. When the switch is closed (during the on-time), the inductor sees the input voltage V_{in} . When the switch is open (during the off-time), the inductor voltage reverses, and it depends on the output voltage of the regulator.

The load current is the current drawn by the load connected to the output of the regulator. This load current affects the behavior of the inductor in the circuit. The load current affects the ripple current (ΔI) through the inductor. Ripple current (ΔI) is the variation (fluctuation) in current through the inductor during each switching cycle. The ripple current (ΔI) calculated represents the peak-to-peak fluctuation in the inductor current. This is the expression for the ripple current (ΔI):

$$\Delta I = \frac{V_{ripple} \times (1-D)}{L \times f} \quad (3)$$

Where D is the duty cycle $[(V_{in}-V_{out})/V_{in}]$, L is the inductance, f is the regulator switching frequency and V_{ripple} is the maximum allowable ripple voltage (50 mV - 150 mV).

Higher load currents typically result in higher ripple currents. The magnitude of the ripple current is directly related to the inductor value and the frequency of the switching action. The LM2576, being a switching regulator, adjusts its duty cycle based on feedback from the output voltage to maintain regulation. As load current changes, the duty cycle and switching frequency might also change to maintain the desired output voltage[3].

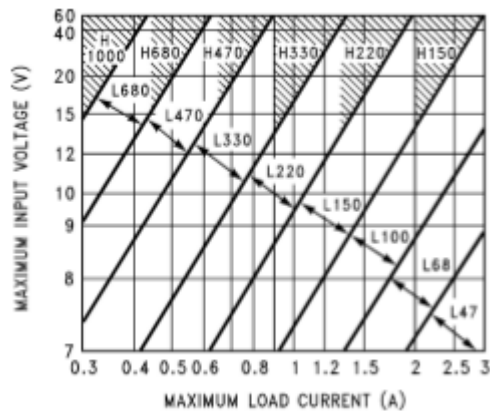


Fig. 12. Relationship between inductor input voltage & load current [3].



Atman Atman, Electrical Engineering student completing the Comprehensive Track. Spring 2024 graduation.



Brandon Lopez is a 22-year old graduating Computer student who is taking a job with Bank of America in Dallas, Tx, as a Software engineer, specializing in Load Balancing Systems.



Isabelle Lebron is a Photonic Engineer who has a drive for leadership and research and will be beginning work at L3 Harris specializing in wireless communications.



Brianna Hurrell is a Photonic Engineer whose passion is research with hopes of continuing that passion within her field.

ACKNOWLEDGEMENT

The authors wish to recognize the assistance and support of Dr. Peter Delfyett, Dr. Kalpathy Sundaram, and Dr. Alfons Schulte in addition to the unwavering support of all of our peers at the University of Central Florida.

REFERENCES

- [1]. Patnaikuni, Patnaik et al. A Comparative Study of Arduino, Raspberry Pi and ESP8266 as IoT Development Board. International Journal of Advanced Research in Computer Science; May/Jun2017, Vol. 8 Issue 5, p2350-2352.
- [2] Spectrometer Design Guide, IBSEN Photonics
- [3]. Texas Instruments Datasheet. SNVS 107G, June 1999. Revised March 2023. Step-down voltage regulator.